Electronic Supplementary Material (ESI) for New Journal of Chemistry.

Boosting the Electrochemical Performance of ZnO Nanomaterial Through Conductive CuS Matrix for Aqueous Supercapacitors

Khalida Mubeen[1,2], Muhammad Zia Ullah Shah*[2,3], Muhammad Sajjad[4,**], Afshan Irshad[1], Zahid Ali[2], Zainab Zafar[5] and A. Shah[2*]

[1]Department of Physics and Mathematics Pakistan Institute of Engineering and Applied Sciences (PIEAS)

[2]National Institute of Lasers and Optronics College, Pakistan Institute of Engineering and Applied Sciences, Nilore, Islamabad 45650, Pakistan

[3]Faculty of Materials Science and Engineering, Kunming University of Science and Technology, Kunming 650093, China

[4]College of Chemistry and Life Sciences, Zhejiang Normal University, Jinhua 321004, P. R China

[5]Experimental Physics Labs, National Centre for Physics, Islamabad, Pakistan

* Corresponding author. attashah168@gmail.com (A.Shah), ziaullah2331@gmail.com (M. Zia. Shah)

**Corresponding author. E-mail address: sajjadfisica@gmail.com (M. Sajjad)

1. Electrochemical properties of the activated carbon

The CV curves of the AC are given in **Fig. S1**. The CV curves in a potential range of -1.0 to 0.0 V at different scans are shown in **Fig. S1a**. The rectangular CV curves confirm the double-layer capacitive performance of the AC. The enlarged CV current response with upsurge scanning rates demonstrates good capacitive and reversibility. The GCD profile was taken at several discharge currents at a similar potential window (-1.0 to 0.0 V), as depicted in **Fig. S2b**. A capacitance at each draft is summarized in **Table S-1**. The capacitance plot, also given in **Fig. S1c,** exhibited a capacitance of 145 F/g and reached 72 F/g. The current increases concerning capacitance due to time constraints.

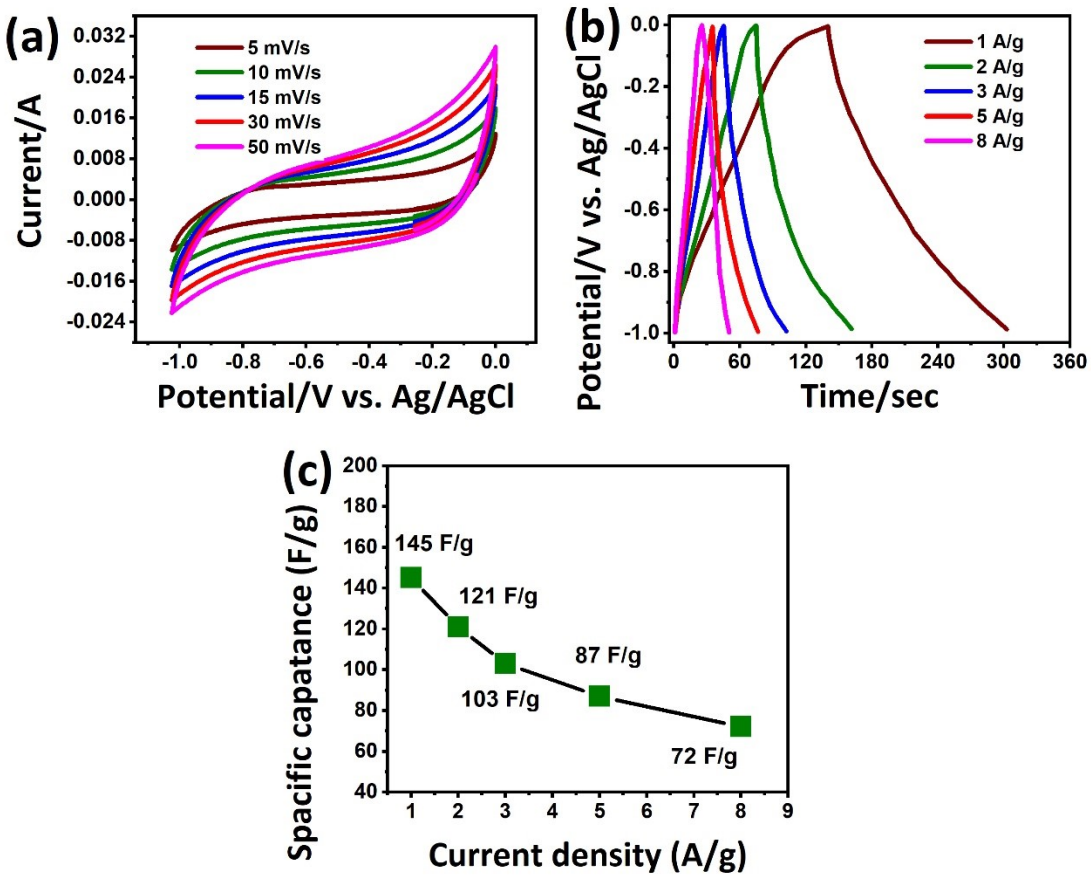

Figure S1. (a) CV curves, (b) GCD profile, and (c) capacitance plot.

The equivalent circuit is provided in **Fig. S2**. As can be seen from the circuit, we observed Rs, Rct, Wuzburg impedance (W), and capacitor in the model, which is consistent with the impedance analysis, as discussed in **Fig. 6**.

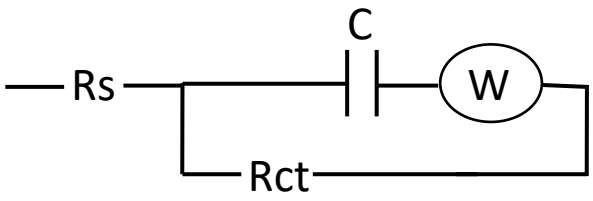

Figure S2. Circuit model of the impedance plot given in **Fig. 6**.

2. Morphology and structural stability after the cycling test

It is essential to thoroughly update the morphological and structural changes after succeeding in long-term stability tests, and the outcomes are given in **Fig. S3**. Notably, the morphological breakdown was noticed by characterizing FESEM micrographs **(Fig. S3a, a1)**. The sample ZnO nanorods and ZnS nanoparticles are broken, and aggregation on the surface progressively restrict the electrolyte ion's movement, hence, a continuous decline in the lifespan of the G-2 electrode. Additionally, the structural and phase purity after the cycling stability showed no apparent structural change observed after the longevity test **(Fig. S3c)**, suggesting the impressive performance of the electrode material.

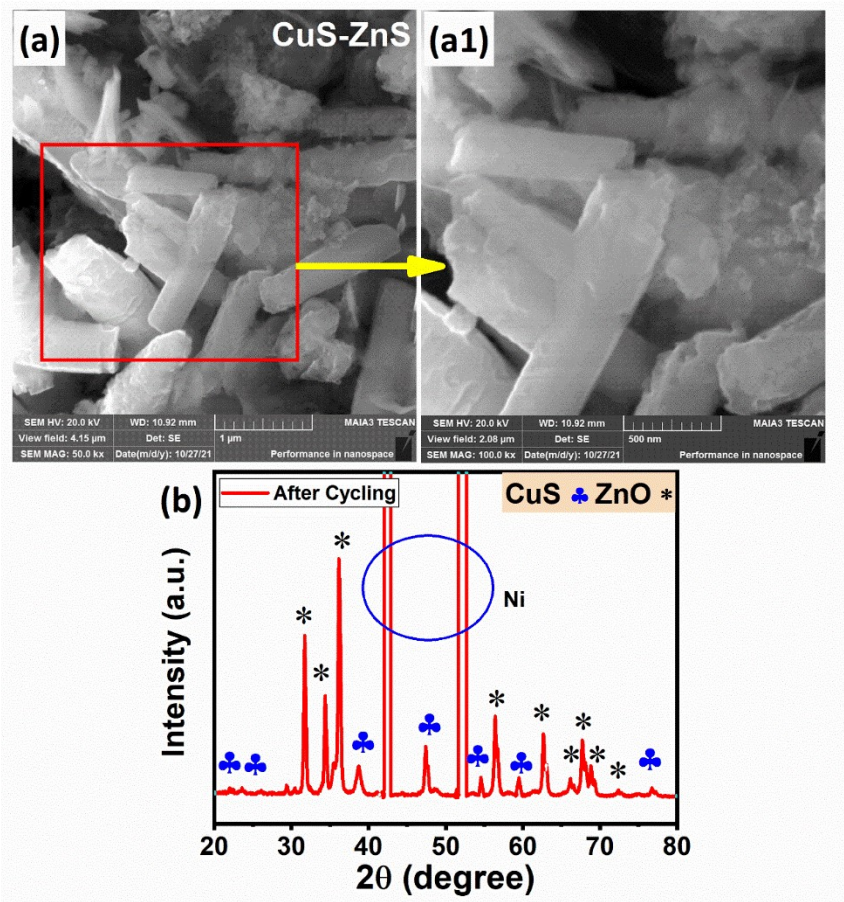

Figure S3. (a, a1) FESEM diagram, and (c) structural features of the active electrode after long-term cycling stability test.

3. Surface chemistry and oxidation states analysis

The sample's oxidation states and surface chemistry were characterized by x-ray photoelectron spectroscopy (XPS) analysis, as depicted in **Fig. S4**. The overall survey spectra of the G-2 sample are demonstrated in **Fig. S4a**. Based on the survey spectrum, S, O, Cu, and Zn peaks are present in the composite. Meanwhile, a C peak is also detected in the range of the substrate when preparing a sample for the XPS measurements. The high-resolution spectrum of the samples is deconvoluted and is separately shown in **Fig. S4b-e**. The Cu 2p spectrum contained two firm peaks into $2p_{3/2}$ and $2p_{1/2}$ with the binding energies of 932.5 eV and 952.8 eV due to Cu^{2+} and Cu^{+} with two shake-up satellite peaks at 942.7 eV and 963.7 eV, as shown in **Fig. S4b**. Also, a Zn 2p orbital further splits into two peaks at 1024.5 eV and 1046.7 eV binding energies **(see Fig. S4c)**. The peak positioned at 161.5 eV, and 162.8 eV arises due to S $2p3_{/2}$ and S $2p_{1/2}$, demonstrating the existence of the sulfur, as displayed in **Fig. S4d**. The oxygen (O) presence was

confirmed from the peaks located at 284.8 eV, and 288 eV was assigned to C=C/C=O, O 1s, binding energy (532.6 eV), as displayed in **Fig. S4e**. According to the brief analysis of the XPS spectrum, it was undoubtedly confirmed that the existence of the elements such as; S, O, Zn, and Cu guarantee the appropriate formation of the composite material.

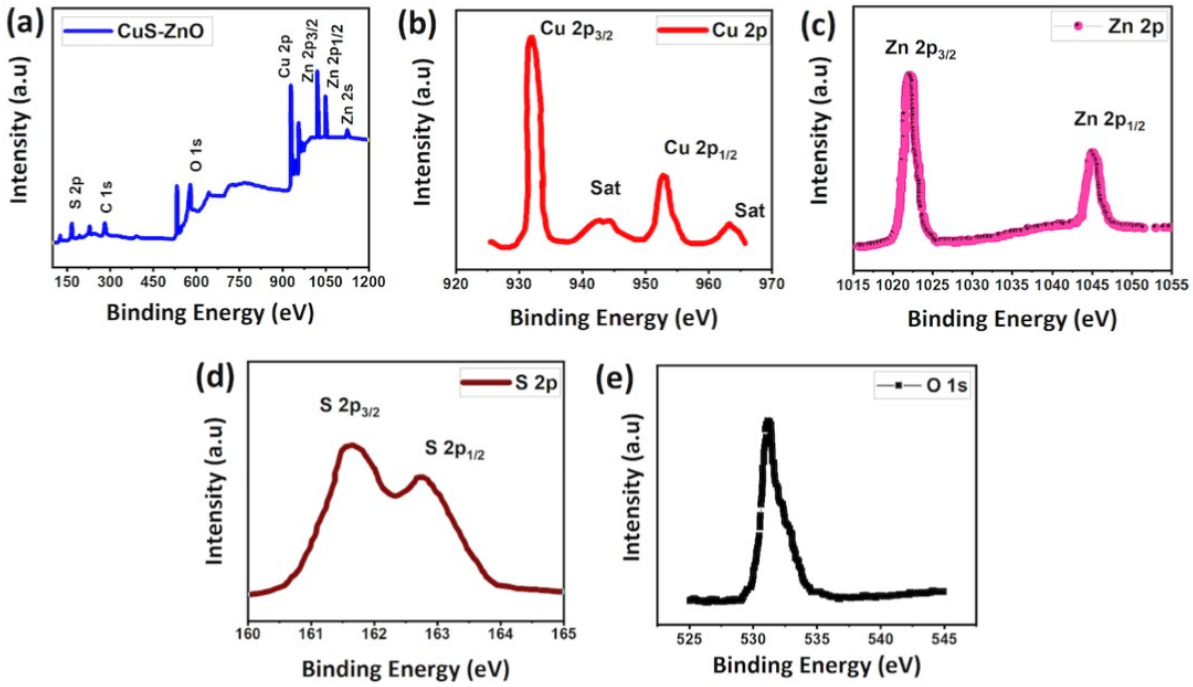

Figure S4. XPS spectrum of the elements, (a) survey spectra, (b) Cu 2p, (c) Zn 2p, (d) S 2p, and (e) O 1s.